NASA Contractor Report 189692

ICASE Report No. 92-39

ICASE

A NUMERICAL RESOLUTION STUDY OF HIGH ORDER
ESSENTIALLY NON-OSCILLATORY SCHEMES APPLIED
TO INCOMPRESSIBLE FLOW

Weinan E
Chi-Wang Shu

NASA

National Aeronautics and
Space Administration

Langley Research Center
Hampton, Virginia 23665-5225

N92-33110

Unclas

0118077

G3/34

(NASA-CR-189692) A NUMERICAL
RESOLUTION STUDY OF HIGH ORDER
ESSENTIALLY NON-OSCILLATORY SCHEMES
APPLIED TO INCOMPRESSIBLE FLOW
Final Report (ICASE) 18 p

A NUMERICAL RESOLUTION STUDY OF HIGH ORDER ESSENTIALLY NON-OSCILLATORY SCHEMES APPLIED TO INCOMPRESSIBLE FLOW[1]

Weinan E[2]

School of Mathematics

Institute for Advanced Study

Princeton, New Jersey 08540

and

Chi-Wang Shu[3]

Division of Applied Mathematics

Brown University

Providence, Rhode Island 02912

ABSTRACT

High order essentially non-oscillatory (ENO) schemes, originally designed for compressible flow and in general for hyperbolic conservation laws, are applied to incompressible Euler and Navier-Stokes equations with periodic boundary conditions. The projection to divergence-free velocity fields is achieved by fourth order central differences through Fast Fourier Transforms (FFT) and a mild high-order filtering. The objective of this work is to assess the resolution of ENO schemes for large scale features of the flow when a coarse grid is used and small scale features of the flow, such as shears and roll-ups, are not fully resolved. It is found that high-order ENO schemes remain stable under such situations and quantities related to large-scale features, such as the total circulation around the roll-up region, are adequately resolved.

i

1 Introduction

In this paper we consider numerically solving the incompressible Navier-Stokes or Euler equations

$$
\begin{aligned}
u_t + u u_x + v u_y &= \mu(u_{xx} + u_{yy}) - p_x \\
v_t + u v_x + v v_y &= \mu(v_{xx} + v_{yy}) - p_y \\
u_x + v_y &= 0
\end{aligned}
\tag{1.1}
$$

or their equivalent conservative form

$$
\begin{aligned}
u_t + (u^2)_x + (uv)_y &= \mu(u_{xx} + u_{yy}) - p_x \\
v_t + (uv)_x + (v^2)_y &= \mu(v_{xx} + v_{yy}) - p_y \\
u_x + v_y &= 0
\end{aligned}
\tag{1.2}
$$

where (u, v) is the velocity vector, p is the pressure, $\mu > 0$ for the Navier-Stokes equations and $\mu = 0$ for the Euler equations. The numerical methods we use are the high-order essentially non-oscillatory (ENO) schemes, originally designed for compressible flow and in general for hyperbolic conservation laws [8], [12]. The equation is defined on the box $[0, 2\pi] \times [0, 2\pi]$ with periodic boundary conditions in both directions. We choose two space dimensions for easy presentation, although our method is also applicable for three space dimensions.

In some sense equations (1.1) are easier to solve numerically than their compressible counter-parts because the latter have solutions containing possible discontinuities (for example shocks and contact discontinuities). However, the solution to (1.1), even if for most cases smooth mathematically, may evolve rather rapidly with time t and may easily become too complicated to be fully resolved on a feasible grid. Traditional linearly stable schemes, such as spectral methods and high-order central difference methods, are suitable for the cases where the solution can be fully resolved, but typically produce signs of instability such as oscillations when small scale features of the flow, such as shears and roll-ups, cannot be adequately resolved on the computational grid (see, for example, the last contour in Fig. 1). Although in principle one can always overcome this difficulty by refining the grid, today's computer capacity seriously restricts the largest possible grid size.

In the last few years there is a lot of activity in designing high-order, nonlinearly stable "shock capturing" schemes for compressible flow and in general for hyperbolic conservation laws. See, for example, [2], [7], [8], [12], and the references listed therein. The philosophy of such schemes is to give up fully resolving rapid transition regions or shocks, just to "capture"

1

them in a stable and somehow globally correct fashion (e.g., with correct shock speed), but at the same time to require a high resolution for the smooth part of the flow. The success of such an approach for the compressible flow is documented by many examples in the literature. One example is the one and two dimensional shock interaction with vorticity or entropy waves [12], [13]. The shock is captured sharply and certain key quantities related to the interaction between the shock and the smooth part of the flow, such as the amplification and generation factors when a wave passes through a shock, are well resolved. Another example is the homogeneous turbulence for compressible Navier-Stokes equations studied in [13]. In one of the test cases, the spectral method can resolve all the scales using a 256^2 grid, while third order ENO with just 64^2 points can adequately resolve certain interesting quantities such as the average fluctuation Mach number and maximum divergence, although it cannot resolve local quantities achieved inside the rapid transition region such as the minimum divergence. The conclusion seems to be that, when fully resolving the flow is either impossible or too costly, a "capturing" scheme such as ENO can be used on a coarse grid to obtain at least some partial information about the flow.

In this paper we perform a similar numerical study for the incompressible equation (1.1), to see what one can get by using the high-order ENO schemes on a coarse grid, without fully resolving the flow. We choose doubly periodic shear layers, used in [1], as our test case. A spectral method with 512^2 points seems able to fully resolve the flow up to $t = 8$, but begins to show signs of underresolution (wriggles in vorticity) thereafter. This indicates the tremendous requirement upon computation resources if one tries to resolve everything in the flow. We then use the third order ENO method (which is fourth order in the L_1 sense) and coarse grids (64^2 and 128^2 points), to assess its resolution. We find that the scheme remains stable for coarse meshes and certain quantities related to the smooth part of the flow, such as the total circulation around the roll-up, are adequately resolved by ENO methods.

A pioneer work in applying shock capturing compressible flow techniques to incompressible flow is by Bell, Colella and Glaz [1], in which they considered a second order Godunov type discretization, investigated the projection into divergence-free velocity fields for general boundary conditions, and discussed accuracy of time discretizations. Since our objective in this paper is to assess the resolution of the ENO method for (1.1), we choose a periodic boundary condition to simplify the projection. General boundary conditions would have to be handled either by more complicated projection [1] or by artificial compressibility methods [4]. We are currently investigating ENO schemes for such cases.

2

2 The ENO Method

We solve (1.2) in its equivalent projection form

$$\begin{pmatrix} u \\ v \end{pmatrix}_t = \mathbf{P}\left[-\begin{pmatrix} u^2 \\ uv \end{pmatrix}_x - \begin{pmatrix} uv \\ v^2 \end{pmatrix}_y + \mu\left(\begin{pmatrix} u \\ v \end{pmatrix}_{xx} + \begin{pmatrix} u \\ v \end{pmatrix}_{yy} \right) \right] \qquad (2.1)$$

where $\mathbf{P}$ is the Hodge projection into divergence-free fields, i.e., if $\begin{pmatrix} \tilde{u} \\ \tilde{v} \end{pmatrix} = \mathbf{P}\begin{pmatrix} u \\ v \end{pmatrix}$, then $\tilde{u}_x + \tilde{v}_y = 0$ and $\tilde{v}_y - \tilde{u}_x = v_y - u_x$. See, e.g., [1]. For the current periodic case the additional condition to obtain a unique projection $\mathbf{P}$ is that the mean values of u and v are preserved, i.e., $\int_0^{2\pi}\int_0^{2\pi} \tilde{u}(x,y)dxdy = \int_0^{2\pi}\int_0^{2\pi} u(x,y)dxdy$ and $\int_0^{2\pi}\int_0^{2\pi} \tilde{v}(x,y)dxdy = \int_0^{2\pi}\int_0^{2\pi} v(x,y)dxdy$.

We use N_x and N_y (even numbers) equally spaced grid points in x and y, respectively. The grid sizes are denoted by $\Delta x = \frac{N_x}{2\pi}$ and $\Delta y = \frac{N_y}{2\pi}$, and the grid points are denoted by $x_i = i\Delta x$ and $y_j = j\Delta y$. The approximated numerical values of u and v at the grid point (x_i, y_j) are denoted by u_{ij} and v_{ij}.

We first describe the numerical implementation of the projection $\mathbf{P}$. In the periodic case this is easily achieved in the Fourier space. We first expand u and v using Fourier collocation:

$$u_N(x,y) = \sum_{l=-\frac{N_y}{2}}^{\frac{N_y}{2}} \sum_{k=-\frac{N_x}{2}}^{\frac{N_x}{2}} \hat{u}_{kl} e^{I(kx+ly)}, \qquad v_N(x,y) = \sum_{l=-\frac{N_y}{2}}^{\frac{N_y}{2}} \sum_{k=-\frac{N_x}{2}}^{\frac{N_x}{2}} \hat{v}_{kl} e^{I(kx+ly)} \qquad (2.2)$$

where $I = \sqrt{-1}$, $\hat{u}_{kl}$ and $\hat{v}_{kl}$ are the Fourier collocation coefficients which can be computed from the point values u_{ij} and v_{ij}, using either FFT or matrix-vector multiplications. The detail can be found in, e.g., [3]. Derivatives, either by spectral method or by central differences, involve only multiplications by factors d_k^x or d_l^y in (2.2) because $e^{I(kx+ly)}$ are eigenfunctions of such derivative operators. For example,

$$d_k^x = Ik, \qquad d_l^y = Il \qquad (2.3)$$

for spectral derivatives;

$$d_k^x = \frac{2I\sin(\frac{k\Delta x}{2})}{\Delta x}, \qquad d_l^y = \frac{2I\sin(\frac{l\Delta y}{2})}{\Delta y} \qquad (2.4)$$

for the second order central differences which, when used twice, will produce the second order central difference approximation $\frac{w_{i+1}-2w_i+w_{i-1}}{\Delta x^2}$ for w_{xx}, and

$$d_k^x = \frac{2I\sqrt{(1-\cos(k\Delta x))(7-\cos(k\Delta x))}}{\Delta x}, \qquad d_l^y = \frac{2I\sqrt{(1-\cos(l\Delta y))(7-\cos(l\Delta y))}}{\Delta y}$$

$$(2.5)$$

3

for the fourth order central differences which, when used twice, will produce the fourth order central difference approximation $\frac{16(w_{i+1}+w_{i-1})-(w_{i+2}+w_{i-2})-30w_i}{12\Delta x^2}$ for w_{xx}. High order filters, such as the exponential filter [10], [9]:

$$\sigma_k^x = e^{-\alpha(\frac{k}{N_x})^{2p}}, \qquad \sigma_l^y = e^{-\alpha(\frac{l}{N_y})^{2p}} \tag{2.6}$$

where $2p$ is the order of the filter and α is chosen so that $e^{-\alpha}$ is machine zero, can be used to enhance the stability while keeping at least $2p$-th order of accuracy. This is especially helpful when the projection $\mathbf{P}$ is used for the under-resolved coarse grid with ENO methods. We use the fourth order projection (2.5) and the filter (2.6) with $2p = 8$ in our calculations. This will guarantee third order accuracy (fourth order in L_1) of the ENO scheme. We will denote this combination (the fourth order projection plus the eighth order filtering) by $\mathbf{P}_4$. To be precise, if $\begin{pmatrix} \tilde{u} \\ \tilde{v} \end{pmatrix} = \mathbf{P}_4 \begin{pmatrix} u \\ v \end{pmatrix}$ and $\hat{u}_{kl}$ and $\hat{v}_{kl}$ are Fourier collocation coefficients of u and v, then the Fourier collocation coefficients of $\tilde{u}$ and $\tilde{v}$ are given by

$$\hat{\tilde{u}} = \sigma_k^x \sigma_l^y \frac{d_l^y(d_l^y\hat{u} - d_k^x\hat{v})}{(d_k^x)^2 + (d_l^y)^2}, \qquad \hat{\tilde{v}} = \sigma_k^x \sigma_l^y \frac{-d_k^x(d_l^y\hat{u} - d_k^x\hat{v})}{(d_k^x)^2 + (d_l^y)^2} \tag{2.7}$$

where σ_k^x and σ_l^y are defined by (2.6) with $2p = 8$, and d_k^x and d_l^y are defined by (2.5).

Next we shall describe the ENO scheme for (2.1). Since (2.1) is equivalent to the non-conservative form (1.1), it is natural to implement upwinding by the signs of u and v, and to implement ENO equation by equation. The r-th order ENO approximation of, e.g., $(u^2)_x$ is thus summarized as follows:

1. Take $f(x) = u^2(x, y)$ with y fixed. We start with the point values $f_i = f(x_i)$;

2. Define a function $h(x)$ satisfying $f(x) = \frac{1}{\Delta x} \int_{x-\frac{\Delta x}{2}}^{x+\frac{\Delta x}{2}} h(\xi)d\xi$, and its primitive $H(x) = \int^x h(\xi)d\xi$. For each $j + \frac{1}{2}$, a $(r + 1)$-th order polynomial $Q_{j+1/2}(x)$ is constructed interpolating $H(x)$ at points near $x_{j+1/2}$. It is remarked in [12] that the Newton divided differences of $H(x)$ are constant multiples of those of $f(x)$ of one order lower. Since we do not need the zeroth order difference, the approximation $Q_{j+1/2}$ of $H(x)$ can be accomplished using the information of f_i only, without explicitly constructing $H(x)$ or its differences;

3. The stencil of the polynomial $Q(x)$ is determined adaptively by upwinding and smoothness of $f(x)$. It starts with either x_j or x_{j+1} according to whether $u \geq 0$ or $u < 0$, then one point to the left or right is added to the stencil each time by comparing the two relevant divided differences and picking the smaller one in magnitude.

4

4. The derivative $f'(x)$ is finally approximated by the conservative difference $\frac{1}{\Delta x}(\hat{f}_{j+1/2} - \hat{f}_{j-1/2})$ where the numerical flux is computed by $\hat{f}_{j+1/2} = \frac{d}{dx}Q(x)|_{x=x_{j+1/2}}$.

5. In the actual coding of the algorithm, undivided differences should be used instead of the divided differences to reduce round-off errors. There are also ways to make the procedure more economical on a vector computer. The details can be found in [13].

The approximation to $(uv)_x$ is the same as above with $f(x) = u(x,y)v(x,y)$, and that for $(uv)_y$ and for $(v^2)_y$ are similar, with upwinding based on v.

There are two ways to handle the second derivative terms for the Navier-Stokes equations. One can absorb them into the convection part and treat them using ENO. For example, $f(x) = u^2(x,y)$ can be replaced by $f(x) = u^2(x,y) - \mu u(x,y)_x$, where $u(x,y)_x$ itself can be obtained using either ENO or central difference of a suitable order. The remaining procedure for computing $f(x)_x$ would be the same as described above. Another simpler possibility is just to use standard central differences (of suitable order) to compute the double derivative terms. Our experience with compressible flow is that there is little difference between the two approaches, especially when the viscosity μ is small.

In the above we have described the discretization for the spatial derivatives

$$L_{ij} \approx \left[-\left(\begin{array}{c} u^2 \\ uv \end{array}\right)_x - \left(\begin{array}{c} uv \\ v^2 \end{array}\right)_y + \mu\left(\left(\begin{array}{c} u \\ v \end{array}\right)_{xx} + \left(\begin{array}{c} u \\ v \end{array}\right)_{yy}\right)\right]_{\substack{x = x_i \\ y = y_j}} . \tag{2.8}$$

Next we use a third order TVD (total variation diminishing) Runge-Kutta method [11] to discretize the resulting ODE:

$$\left(\begin{array}{c} u \\ v \end{array}\right)_t = \mathbf{P}_4 L_{ij} \tag{2.9}$$

obtaining:

$$
\begin{aligned}
\left(\begin{array}{c} u \\ v \end{array}\right)^{(1)} &= \mathbf{P}_4\left[\left(\begin{array}{c} u \\ v \end{array}\right)^n + \Delta t L_{ij}^n\right] \\
\left(\begin{array}{c} u \\ v \end{array}\right)^{(2)} &= \mathbf{P}_4\left[\frac{3}{4}\left(\begin{array}{c} u \\ v \end{array}\right)^n + \frac{1}{4}\left(\begin{array}{c} u \\ v \end{array}\right)^{(1)} + \frac{1}{4}\Delta t L_{ij}^{(1)}\right] \\
\left(\begin{array}{c} u \\ v \end{array}\right)^{n+1} &= \mathbf{P}_4\left[\frac{1}{3}\left(\begin{array}{c} u \\ v \end{array}\right)^n + \frac{2}{3}\left(\begin{array}{c} u \\ v \end{array}\right)^{(2)} + \frac{2}{3}\Delta t L_{ij}^{(2)}\right]
\end{aligned}
\tag{2.10}
$$

Notice that we have used the property $P_4 \circ P_4 = P_4$ in obtaining the discretization (2.10) from (2.9).

This explicit time discretization is expected to be nonlinearly stable under the CFL condition

$$\Delta t \left[\max_{i,j} \left(\frac{|u_{ij}|}{\Delta x} + \frac{|v_{ij}|}{\Delta y} \right) + 2\mu \left(\frac{1}{\Delta x^2} + \frac{1}{\Delta y^2} \right) \right] \leq 1 \qquad (2.11)$$

(see [11]). For small μ (which is the case we are interested in) this is not a serious restriction on Δt.

3 Numerical Results

We present two numerical examples in this section.

Example 1: This example is used to check the third order accuracy of our ENO scheme for smooth solutions. We first take the initial condition as

$$u(x, y, 0) = -\cos(x)\sin(y), \qquad v(x, y, 0) = \sin(x)\cos(y) \qquad (3.1)$$

which was used in [5]. The exact solution for this case is known:

$$u(x, y, t) = -\cos(x)\sin(y)e^{-2\mu t}, \qquad v(x, y, t) = \sin(x)\cos(y)e^{-2\mu t} \qquad (3.2)$$

We take $\Delta x = \Delta y = \frac{1}{N}$ with $N = 32, 64, 128$ and 256. The solution is computed up to $t = 2$ and the L_2 error and numerical order of accuracy are listed in Table 3.1. For the $\mu = 0.05$ case, we list results both with fourth order central approximation to the double derivative terms (central) and with ENO to handle the double derivative terms by absorbing them into the convection part (ENO). We can clearly observe fully third order accuracy (actually better in many cases because the spatial ENO is fourth order in the L_1 sense) in this table.

Table 3.1: Accuracy of ENO Schemes for (3.1)

N	$\mu = 0$		$\mu = 0.05$, central		$\mu = 0.05$, ENO	
	L_2 error	order	L_2 error	order	L_2 error	order
32	9.10(-4)		5.28(-4)		4.87(-4)	
64	5.73(-5)	3.99	3.20(-5)	4.04	3.09(-5)	3.98
128	3.62(-6)	3.98	1.93(-6)	4.05	1.89(-6)	4.03
256	2.28(-7)	3.99	1.18(-7)	4.03	1.16(-7)	4.03

We then take the initial condition as

$$u(x,y,0) = -\sin^2(x)\sin(2y), \qquad v(x,y,0) = \sin(2x)\sin^2(y) \qquad (3.3)$$

which was used in [1]. We again take $\Delta x = \Delta y = \frac{1}{N}$ with $N = 16, 32, 64, 128$ and 256 and compute the solution up to $t = 2$. However, this time the exact solution is unknown. As in [1], we test the accuracy by computing the L_2 difference between the solutions at the grid sizes $2\Delta x$ and Δx, on the coarser grid. If $w_{\Delta x} = w + C\Delta x^r + O(\Delta x^{r+1})$, then this difference $w_{2\Delta x} - w_{\Delta x} = (2^r - 1)C\Delta x^r + O(\Delta x^{r+1})$ would predict the correct asymptotic order of accuracy r and the error itself on the finer grid multiplied by $2^r - 1$. The result is summarized in Table 3.2, where $\mathbf{w} = (u, v)^T$ and L_2 diff$= \|\mathbf{w}_{2\Delta x} - \mathbf{w}_{\Delta x}\|_{L_2}$. In this table the estimated order and error are obtained using the remarks above. For $\mu = 0.05$, we have again provided results both with fourth order central approximation to the double derivative terms (central) and with ENO to handle the double derivative terms by absorbing them into the convection part (ENO). The result in Table 3.2 reconfirms better than third order accuracy for the third order ENO scheme.

Table 3.2: Accuracy of ENO Schemes for (3.3)

N	$\mu = 0$			$\mu = 0.05$, central			$\mu = 0.05$, ENO		
	L_2 diff	order	error	L_2 diff	order	error	L_2 diff	order	error
32	1.14(-1)			3.20(-2)			3.60(-2)		
64	1.40(-2)	3.02	1.96(-3)	2.78(-3)	3.52	2.66(-4)	2.93(-3)	3.62	2.60(-4)
128	1.46(-3)	3.26	1.69(-4)	1.81(-4)	3.94	1.26(-5)	1.80(-4)	4.02	1.18(-5)
256	1.11(-4)	3.77	8.78(-6)	1.09(-5)	4.06	6.91(-7)	1.10(-5)	4.04	7.15(-7)

Example 2: This is our test example to study resolution of ENO schemes when the grid is coarse. It is a double shear layer taken from [1]:

$$u(x,y,0) = \begin{cases} \tanh((y - \pi/2)/\rho) & y \le \pi \\ \tanh((3\pi/2 - y)/\rho) & y > \pi \end{cases} \qquad v(x,y,0) = \delta\sin(x) \qquad (3.4)$$

where we take $\rho = \pi/15$ and $\delta = 0.05$. The Euler equations ($\mu = 0$) are used for this example. The solution quickly develops into roll-ups with smaller and smaller scales, so on any fixed grid the full resolution is lost eventually. For example, the expensive run we performed using 512^2 points for the spectral collocation code (with a 18-th order filter (2.4)) seems able to resolve the solution fully up to $t = 8$, then begins to lose resolution as indicated by the wriggles in the vorticity contour at $t = 10$ (the last contour in Fig. 1). On the other hand, the ENO runs with 64^2 and 128^2 points produces smooth, stable results (Fig. 2 and 3). Apparently with these coarse grids the full structure of the roll-up is not resolved. However, when we compute the total circulation

7

$$c_\Omega = \int_\Omega \omega(x,y)dxdy = \int_{\partial\Omega} udx + vdy \qquad (3.5)$$

around the roll-up by taking $\Omega = [\frac{\pi}{2}, \frac{3\pi}{2}] \times [0, 2\pi]$ and using the rectangular rule (which is infinite order accurate for the periodic case) on the line integrals at the right-hand-side of (3.5), we can see that this number is resolved much better than the roll-up itself (see Table 3.3).

Table 3.3: Resolution of the Total Circulation

t	2	4	6	8	10
ENO 64^2	0.87300	3.07100	7.16889	9.88063	10.90122
ENO 128^2	0.87452	2.97810	7.30999	10.34414	11.79418
spectral 512^2	0.87433	2.98029	7.28308	10.46212	11.85875

4   Concluding Remarks

High order ENO schemes can be applied to the incompressible Euler and Navier-Stokes equations to obtain stable, under-resolved results on a coarse grid. Some global quantities such as the circulation around the roll-up region can be faithfully resolved.

References

[1] J. Bell, P. Colella and H. Glaz, *A Second Order Projection Method for the Incompressible Navier-Stokes Equations*, J. Comput. Phys., v85, 1989, pp.257-283.

[2] P. Colella and P. Woodward, *The Piecewise Parabolic Method (PPM) for Gas-Dynamical Simulations*, J. Comput. Phys., v54, 1984, pp.174-201.

[3] C. Canuto, M.Y. Hussaini, A. Quarteroni and T. A. Zang, *Spectral Methods in Fluid Dynamics*, Springer-Verlag, 1988.

[4] A. Chorin, *A Numerical Method for Solving Incompressible Viscous Flow Problems*, J. Comput. Phys., v2, 1967, pp.12-26.

[5] A. Chorin, *Numerical Solution of the Navier-Stokes Equations*, Math. Comput., v22, 1968, pp.745-762.

[6] D. Gottlieb and S. Orszag, *Numerical Analysis of Spectral Methods: Theory and Applications*, v26, SIAM-CBMS, Philadephia, 1977.

[7] A. Harten, *High Resolution Schemes for Hyperbolic Conservation Laws*, J. Comput. Phys., v49, 1983, pp.357-393.

[8] A. Harten, B. Engquist, S. Osher and S. Chakravarthy, *Uniformly High Order Accurate Essentially Non-Oscillatory Schemes, III*, J. Comput. Phys., v71, 1987, pp.231-303.

[9] D. A. Kopriva, *A Practical Assessment of Spectral Accuracy for Hyperbolic Problems with Discontinuities*, J. Sci. Comput., v2, 1987, pp.249-262.

[10] A. Majda, J. McDonough and S. Osher, *The Fourier Method for Nonsmooth Initial Data*, Math. Comput., v32, 1978, pp.1041-1081.

[11] C.-W. Shu and S. Osher, *Efficient Implementation of Essentially Non-Oscillatory Shock Capturing Scheme*, J. Comput. Phys., v77, 1988, pp.439-471.

[12] C.-W. Shu and S. Osher, *Efficient Implementation of Essentially Non-Oscillatory Shock Capturing Scheme, II*, J. Comput. Phys., v83, 1989, pp.32-78.

[13] C.-W. Shu, T.A. Zang, G. Erlebacher, D. Whitaker and S. Osher, *High Order ENO Schemes Applied to Two- and Three-Dimensional Compressible Flow*, Appl. Numer. Math., v9, 1992, pp.45-71.

Figure 1: The vorticity contour for Example 2 at $t = 4, 6, 8, 10$. Spectral method with 512^2 points.
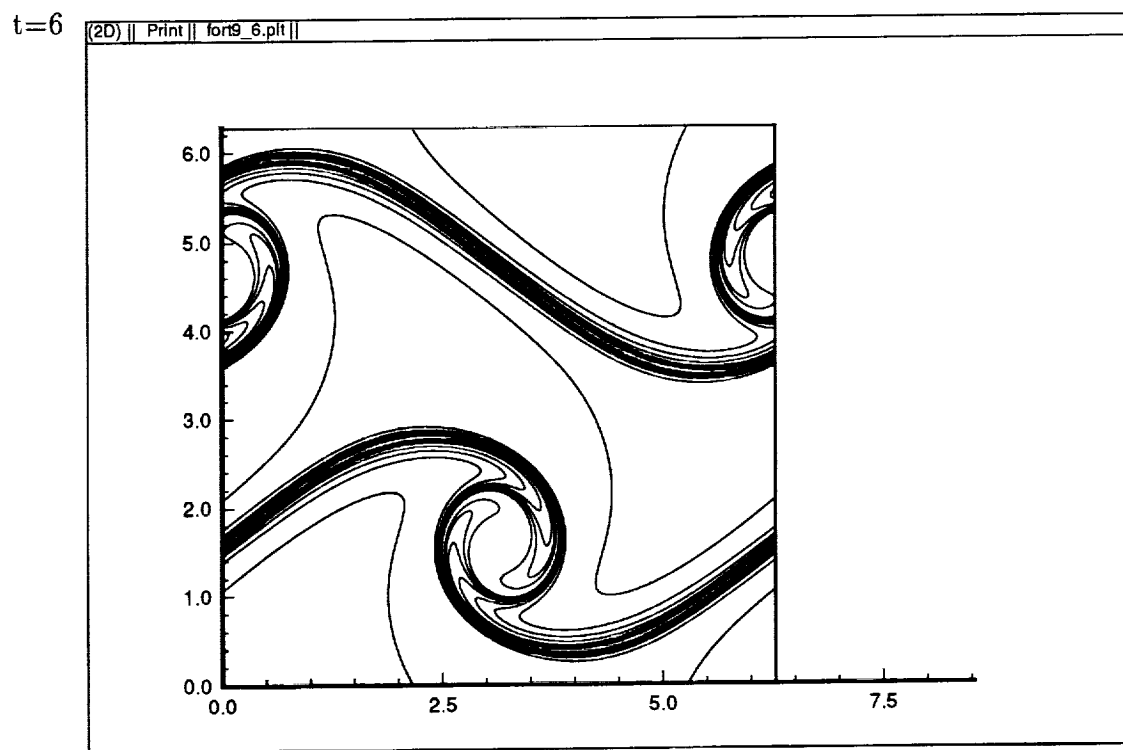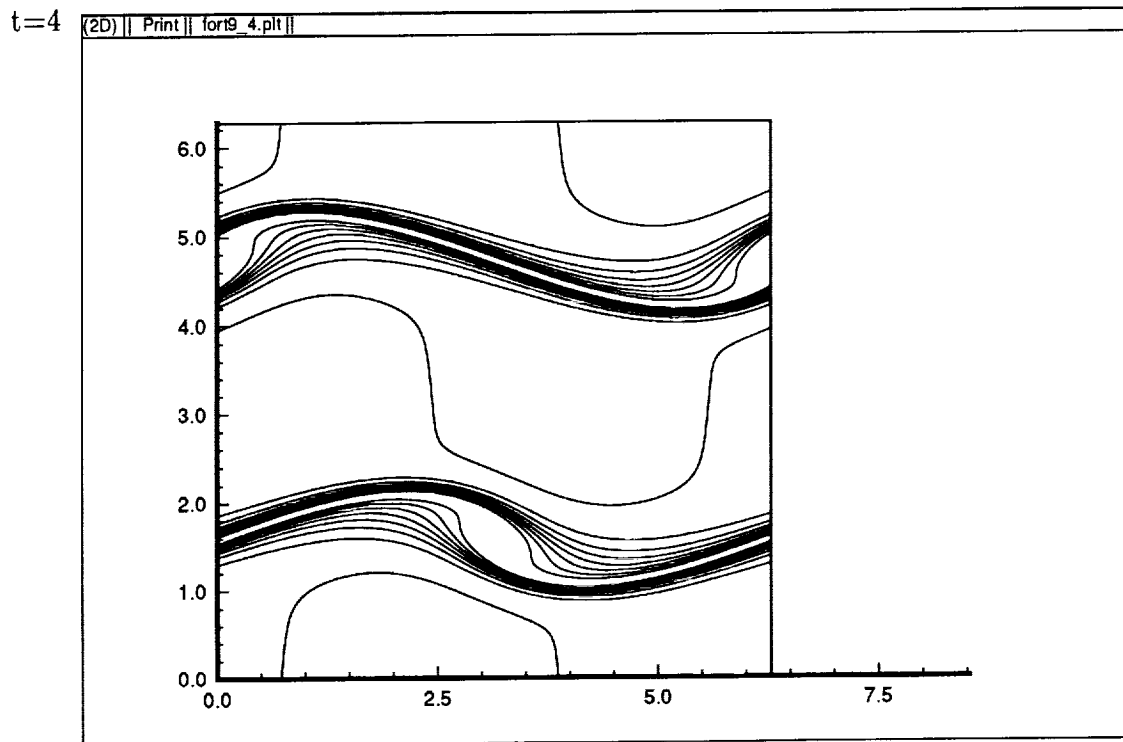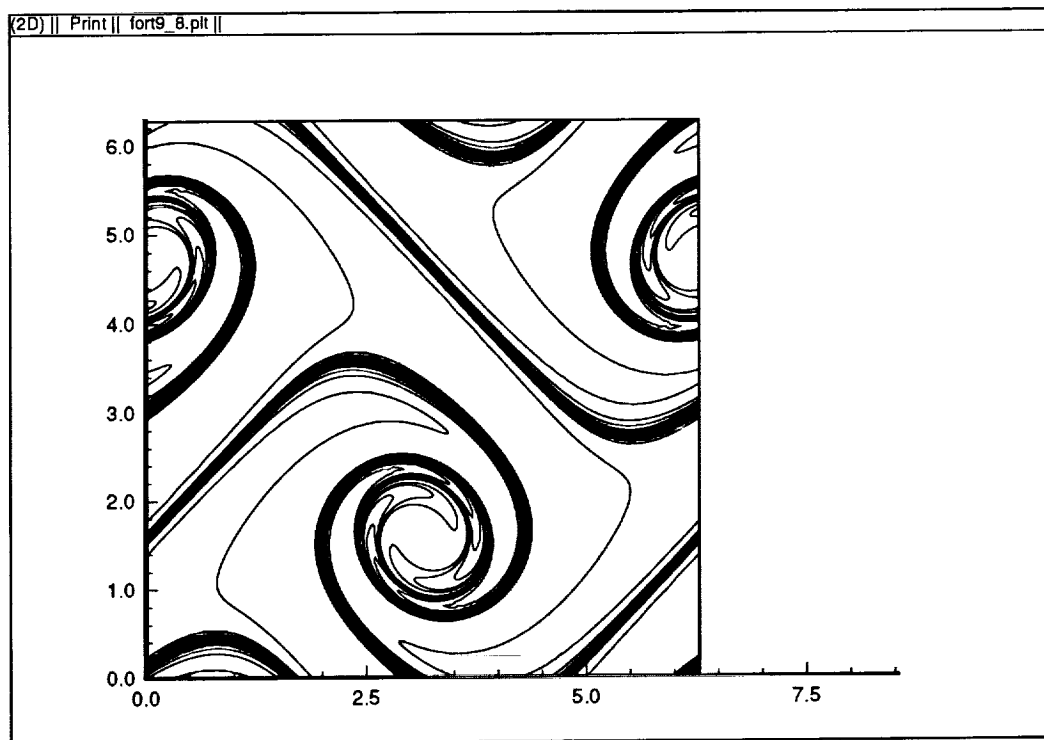
t=4

t=6

Figure 1 continued:

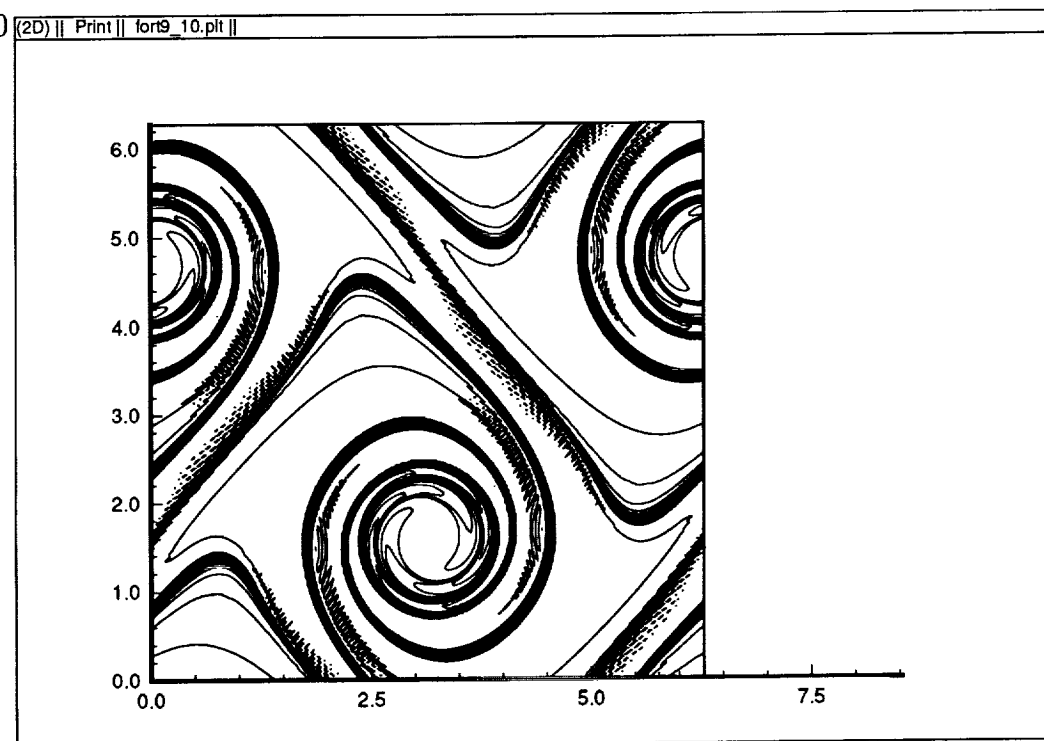t=8 (2D) || Print || fort9_8.plt ||

t=10 (2D) || Print || fort9_10.plt ||
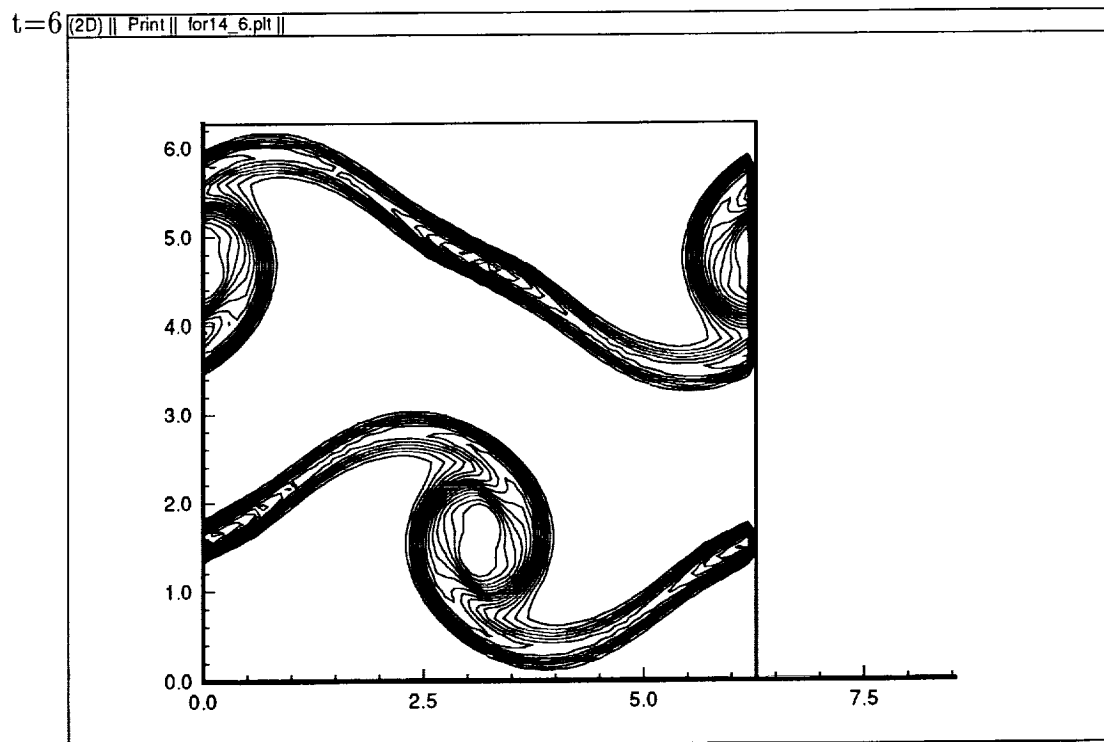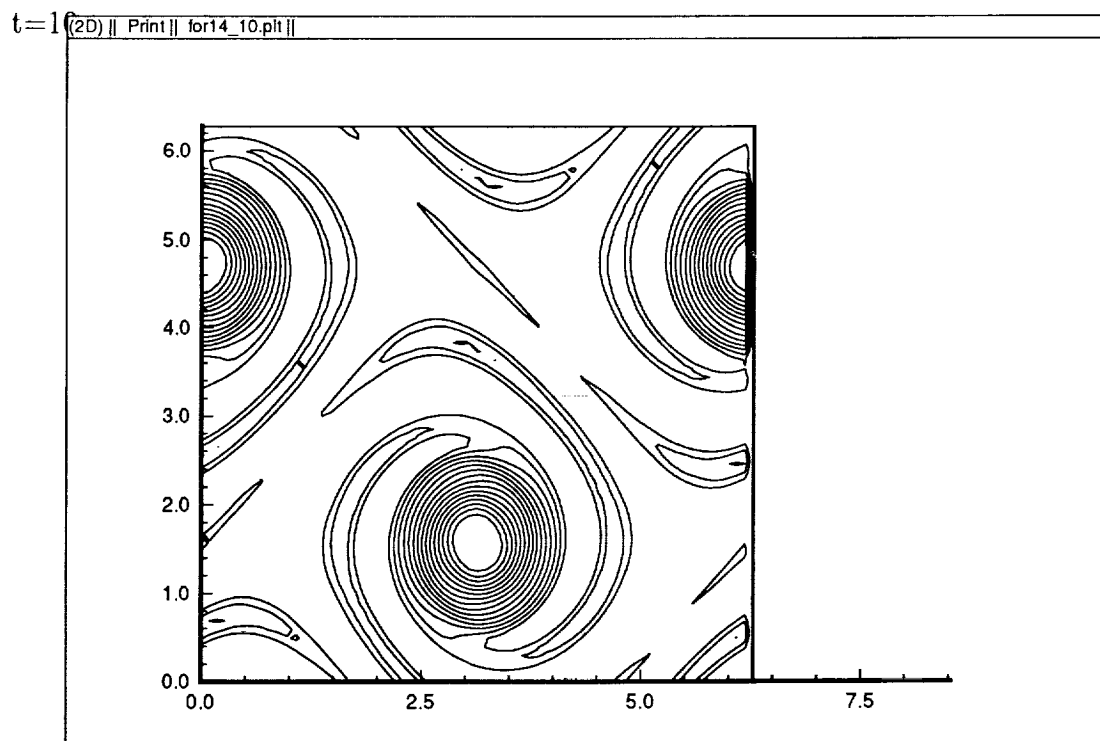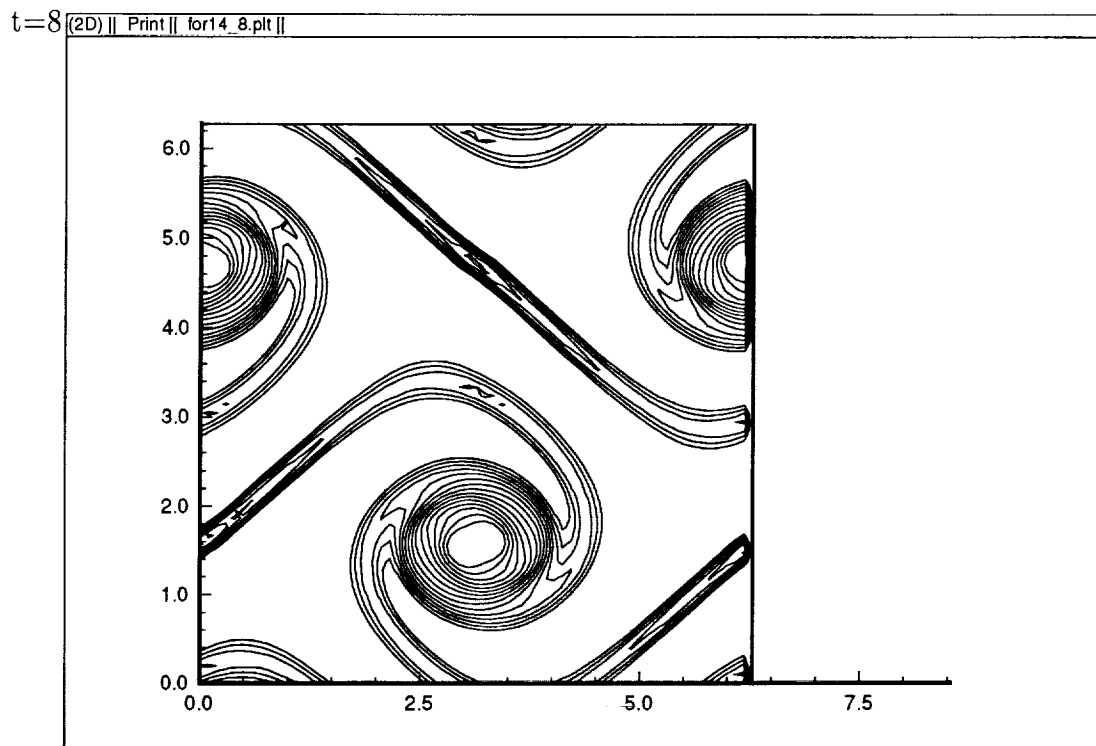
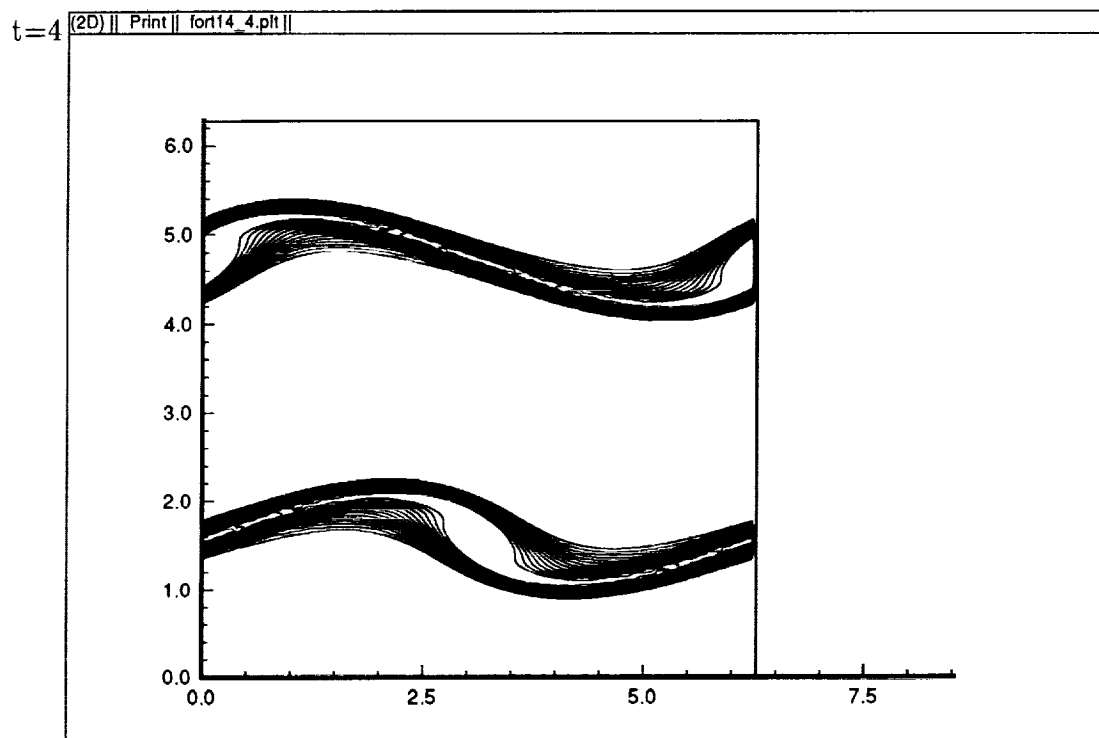Figure 2: The vorticity contour for Example 2 at $t = 4, 6, 8, 10$. ENO method with 64^2 points.

t=4 | (2D) || Print || for14_4.plt ||

t=6 | (2D) || Print || for14_6.plt ||

Figure 2 continued:

$t=8$ (2D) ‖ Print ‖ for14_8.plt ‖

$t=10$ (2D) ‖ Print ‖ for14_10.plt ‖

13
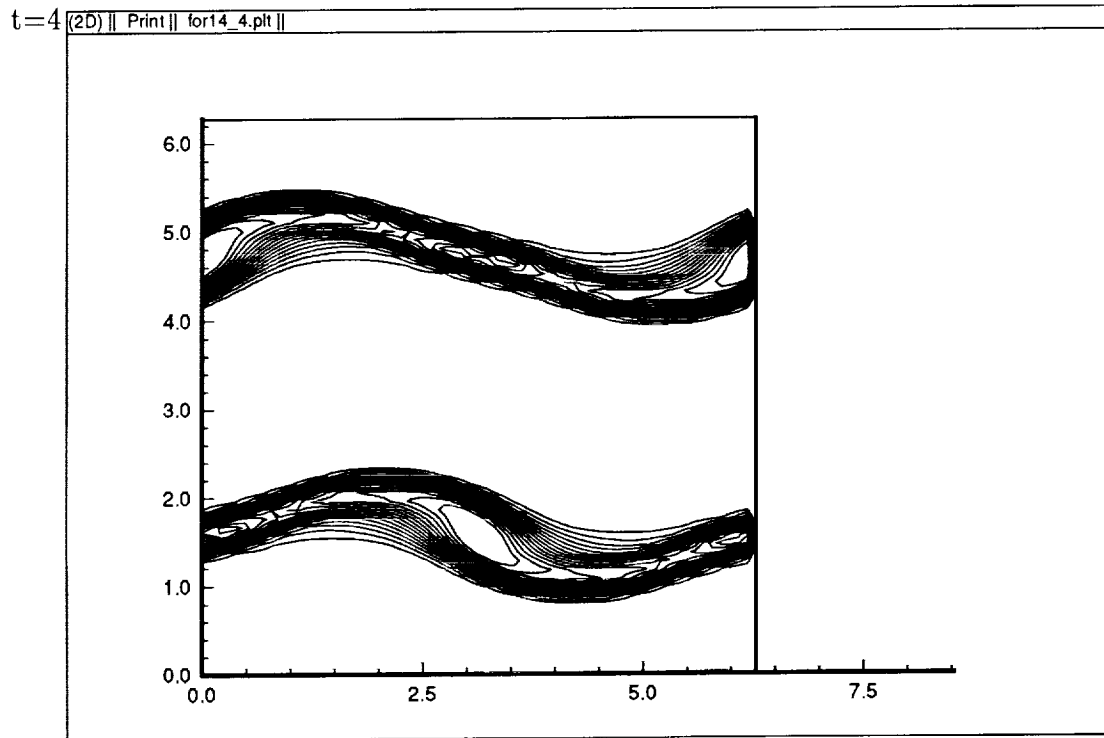
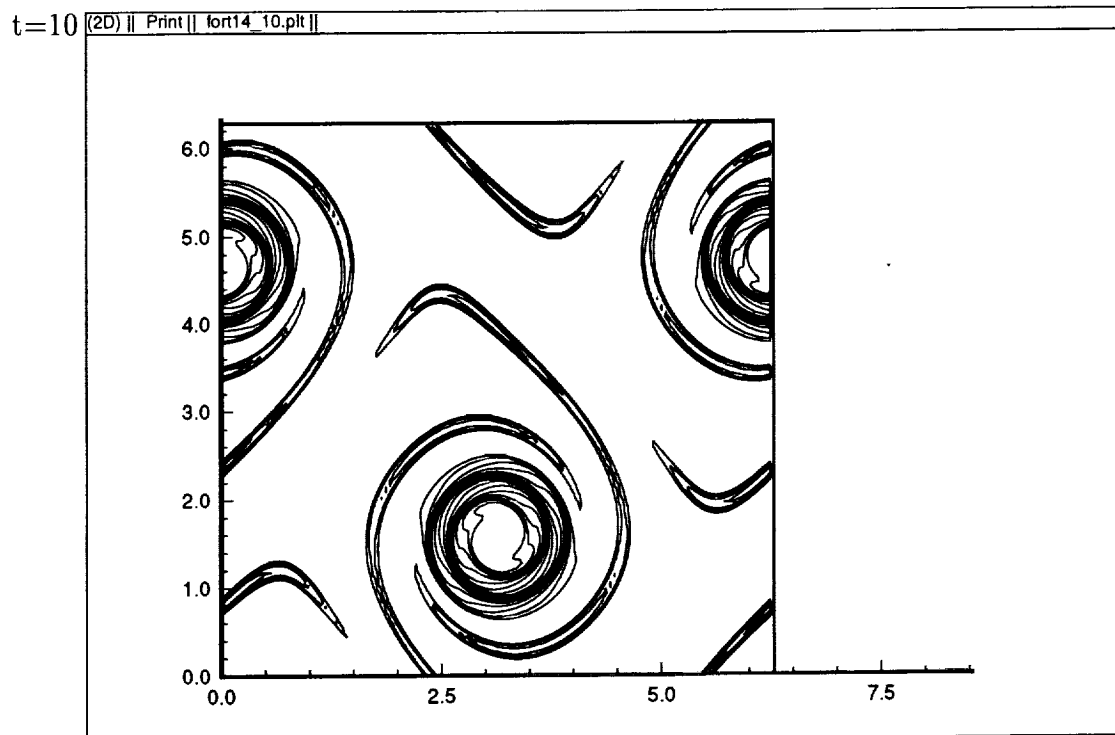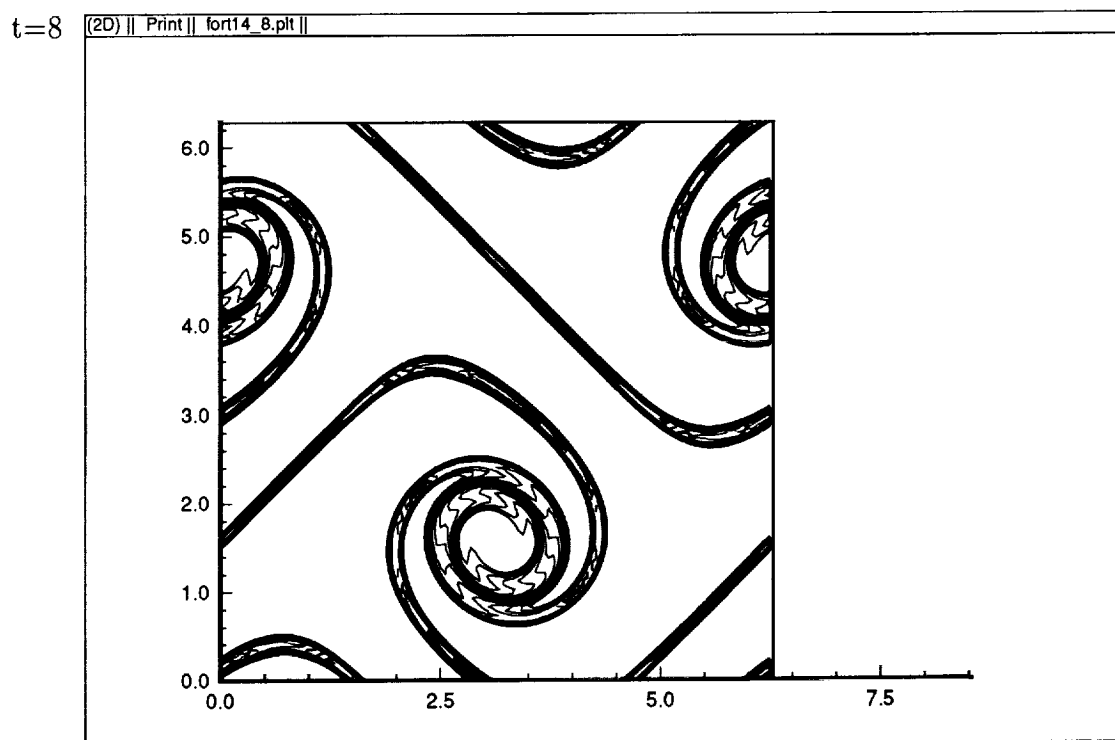Figure 3: The vorticity contour for Example 2 at $t = 4, 6, 8, 10$. ENO method with 128^2 points.

t=4

t=6

Figure 3 continued:

t=8   [2D] || Print || fort14_8.plt ||

t=10   [2D] || Print || fort14_10.plt ||
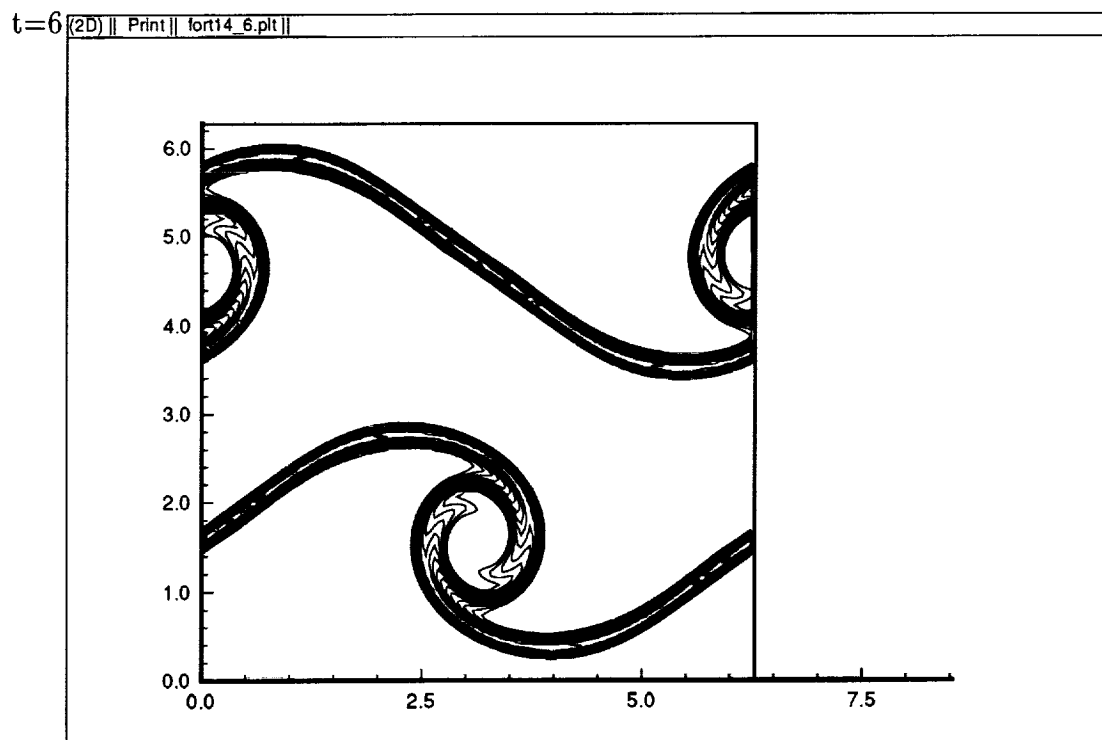
REPORT DOCUMENTATION PAGE

1. AGENCY USE ONLY (Leave blank)	2. REPORT DATE August 1992	3. REPORT TYPE AND DATES COVERED Contractor Report

4. TITLE AND SUBTITLE A NUMERICAL RESOLUTION STUDY OF HIGH ORDER ESSENTIALLY NON-OSCILLATORY SCHEMES APPLIED TO INCOMPRESSIBLE FLOW	5. FUNDING NUMBERS C NAS1-18605 C NAS1-19480
6. AUTHOR(S) Weinan E Chi-Wang Shu	WU 505-90-52-01

7. PERFORMING ORGANIZATION NAME(S) AND ADDRESS(ES) Institute for Computer Applications in Science and Engineering Mail Stop 132C, NASA Langley Research Center Hampton, VA 23665-5225	8. PERFORMING ORGANIZATION REPORT NUMBER ICASE Report No. 92-39

9. SPONSORING/MONITORING AGENCY NAME(S) AND ADDRESS(ES) National Aeronautics and Space Administration Langley Research Center Hampton, VA 23665-5225	10. SPONSORING/MONITORING AGENCY REPORT NUMBER NASA CR-189692 ICASE Report No. 92-39

11. SUPPLEMENTARY NOTES

Langley Technical Monitor: Michael F. Card   Submitted to Journal of Computational Physics
Final Report

12a. DISTRIBUTION/AVAILABILITY STATEMENT Unclassified - Unlimited Subject Category 34, 64	12b. DISTRIBUTION CODE

13. ABSTRACT *(Maximum 200 words)*

High order essentially non-oscillatory (ENO) schemes, originally designed for compressible flow and in general for hyperbolic conservation laws, are applied to incompressible Euler and Navier-Stokes equations with periodic boundary conditions. The projection to divergence-free velocity fields is achieved by fourth order central differences through Fast Fourier Transforms (FFT) and a mild high-order filtering. The objective of this work is to assess the resolution of ENO schemes for large scale features of the flow when a coarse grid is used and small scale features of the flow, such as shears and roll-ups, are not fully resolved. It is found that high-order ENO schemes remain stable under such situations and quantities related to large-scale features, such as the total circulation around the roll-up region, are adequately resolved.

14. SUBJECT TERMS incompressible flow; essentially non-oscillatory schemes; high order accuracy	15. NUMBER OF PAGES 17
	16. PRICE CODE A03

17. SECURITY CLASSIFICATION OF REPORT Unclassified	18. SECURITY CLASSIFICATION OF THIS PAGE Unclassified	19. SECURITY CLASSIFICATION OF ABSTRACT	20. LIMITATION OF ABSTRACT